A Full-Field Calibration Approach on Material Parameter Identification

A Full-Field Calibration Approach on Material Parameter Identification

Cavariani, S.[1], Scattina, A.[1], Scalera, S.[2], Bianco, S.[3], D'Aiuto, F.[3], De Caro, D.[3], Ghisleri, D.[3], Luera, A.[3], Tedesco, M.M.[3], Ilg, C.[4]

[1]Politecnico di Torino, Corso Duca degli Abruzzi 24, Turin, Italy
[2]DYNAmore Italia srl, Piazza Castello 139 Turin, Italy
[3]C.R.F. S.C.p.A, Corso Settembrini 40, Turin, Italy
[4]DYNAmore GmbH, Industriestrasse 2, 70569 Stuttgart, Germany

1 Introduction

Nowadays the possibility to accurately simulate steel alloys is crucial to expect accurate results in crash analysis. Just as much as welding spots, innovative materials like polymers or composites more predictive steel material models are continually sought after throughout the industry.
Complex models require a significant effort to calibrate them to the physical behaviour of the materials, but they can perform better. This work will evaluate and compare different techniques to characterize materials for finite element simulations.

2 Objectives

The objective of this work is to analyse the effectiveness of a new material calibration technique, available in LS-OPT since the version 6, called "Full field calibration" (FFC) [1]. It is based on the application of the digital image correlation to the experimental tests.
The typical operation in a steel testing application would employ a universal testing machine together with an extensometer to measure the tensile load and the displacements during a tensile test. The displacements measured are then used to compute the average strain between the measuring points. In this work, the analysis carried out this way will be referred to as "Standard" (ST).
Due to the advent of new strain measurement technologies, such as the digital image correlation it is now possible to acquire and analyse the strain field, from the local displacements on the surface. The possibility to include in the material model information coming from the whole analysed piece, or at least from a significant region of it, allows for a richer description of its behaviour. The "Full field Calibration" technique also permits to inspect the necking area, which is affected by the highest strains and strain gradient during the tests.

In this work, the material characterization will be split in two parts: the determination of the yield curve of the materials and the optimization of a failure model present in the LS-DYNA, named GISSMO [2].
To determine the yield curve only one tensile test is needed. Two materials were tested, a martensitic high strength steel (MS1500) and a more ductile dual phase steel (DP800). This last material is often utilized for automotive applications.
To tune the failure model GISSMO, the test specimens need to span a wide range of triaxiality [3]. For this reason, the results of the tests *shear 0°*, *notched*, *double notched*, *tensile* were used in the calibration, but only for the MS1500, because only the specimen for the *tensile* test was available for the DP800.
The determination of the yield curves and of the GISSMO parameters will be performed with both approaches, FFC and ST, to highlight the strengths and the weakness of each of them.

3 Yield Curve

The yield curve regulates the behaviour of the material in the plastic domain [4] and it can be uniquely determined from the engineering stress-strain curve up to the beginning of the localization in the material [1]. Up to that point the load needed to progress with the deformation of the piece monotonically grows. When the load on the cross-section reaches its maximum, the strain field inside the test specimen is no longer uniform and there ceases to be a univocal correspondence between the strains and the loads. The strains become a function of the measuring gauge length. Beyond this point, the extrapolation of the yield curve was performed following the approach proposed by Hockett & Sherby [5]:

$$\sigma_y = A - B \cdot e^{\left(-C \cdot \epsilon_{pl}^{N}\right)} \quad (1)$$

This model presents four variables of which two are bound due to C^1 continuity, leaving C and N free to be used in the optimization [6]. The next two sections describe how the two different approaches search for the optimal pair of parameters.

3.1 Standard

A LS-OPT project is created to iteratively simulate the experimental test with different values of C and N. To find the best pair of parameters, LS-OPT compares the experimental engineering force-strain curve to the one evaluated with the simulation. LS-OPT explores the design space, which is a 2D space made by C and N, to minimize the difference between the simulated and the measured engineering force-strain curve. The two curves are compared using the "partial curve matching" algorithm [7]. LS-OPT builds a metamodel using the simulations and the optimum is searched on it with a sequential strategy with domain reduction [8].

3.2 Full field calibration

In this case the Hockett & Sherby model is optimized in the same manner but using a different objective. The strain field is recorded during the experimental tensile test and it is compared with the strain path that is simulated. The experimental strain field is obtained using the correlation software "GOM aramis". Aramis outputs an object named "hyper-curve" [9] that is a family of curves, all with the same load profile but with different strains depending on the position. In this way, the strain field of the specimen is represented. The hyper-curve is compared by LS-OPT with the corresponding one generated from the simulation's *d3plot.* The objective of the optimization is to find the combination of C and N that minimizes the difference between the two strain fields over time. The same structure and options were used to generate the optimization as in the ST approach.

Fig.1: LS-OPT user interface showing how the strain field comparison is performed.

3.3 Results

To determine the yield curve only the tensile test for each material was analysed and simulated. The figure 2 presents the results of the optimizations.

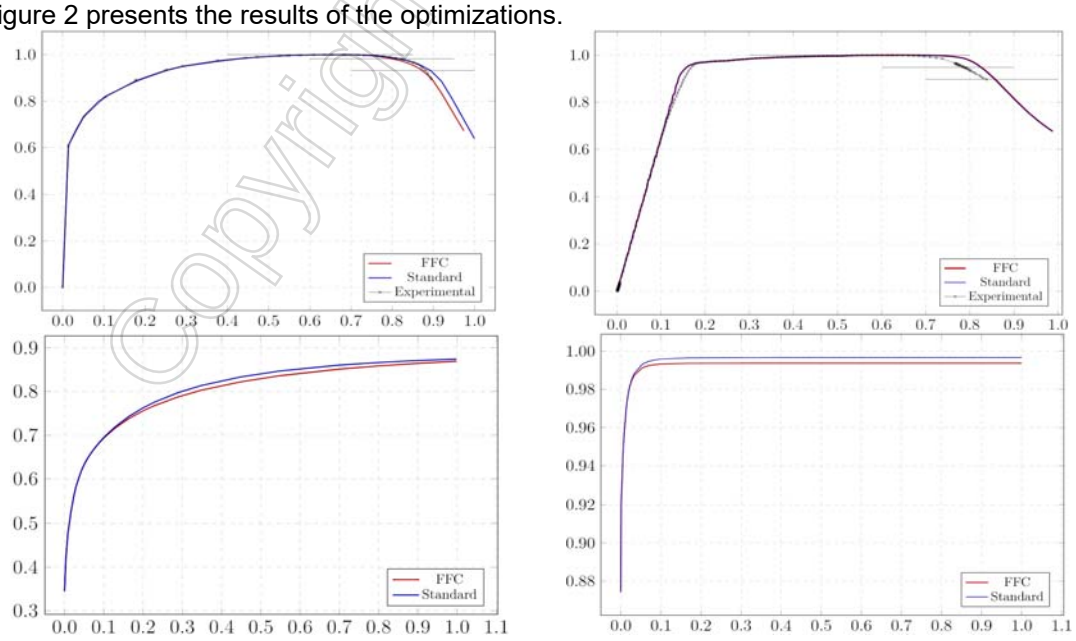

Fig.2: The first row of graphs shows engineering stress strain curves of the material compared with the ones simulated with different yield curves: DP800 on the left, MS1500 on the right. Below following the same order, are the yield curves that were used in the simulations.

Across the two materials the results of the different methods are coherent, with the yield curves resulted from the Standard and the Full field optimization being very close for both materials. Table 1 presents the maximum strains measured experimentally alongside the values measured in the simulations, for both materials. The load levels in comparison are indicated in figure 3 with the horizontal black lines.

Comparison load	DIC	FFC	Standard
Max. Load	0.14	0.14	0.14
(Max. Load)·0.98	0.32	0.40	0.44
(Max. Load)·0.93	0.37	0.52	0.57

Comparison load	DIC	FFC	Standard
Max. Load	0.052	0.0327	0.0338
(Max. Load)·0.95	0.192	0.220	0.299
(Max. Load)·0.9	0.313	0.358	0.373

Table 1: Maximum measured strains for the DP800, on the left, and MS1500, on the right.

The FFC approach presents the best predictability in terms of strains, even if its yield curve is very similar to the one coming from the ST approach. These results can be explained by the different objective employed in the optimizations. The ST approach utilizes the engineering curve. Indeed, the results is more accurate in reproducing the experimental curve in particular for the DP800. The FFC approach minimizes the differences in the strain field and while it performs worse on the engineering curve, it presents a superior predictability on the actual strains inside the piece. Using the engineering stress-strain curve as an objective of the optimization, it could be non-representative when the actual target is reproducing the physics of the material that is the strain field.

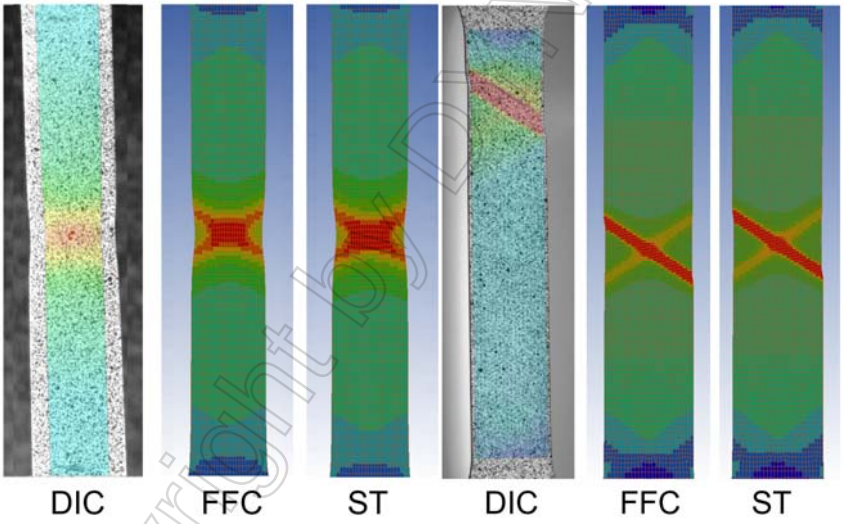

Fig.3: Strain fields comparison: DP800 on the left and MS1500 on the right

The two methods achieve slightly different results, however evaluating how much this difference could influence a full crash application is impossible without additional testing. A possible solution could be the simulation of a three-point bending of a component. Based on the authors' experiences, at this point in time, it is believed that the difference between the FFC and the ST towards the determination of the yield curve is negligible.

To further analyse the comparison, there is a difference in the time and the complexity of the experimental tests, and the test results elaboration, which are more demanding for the FFC approach. Other aspect that weights against the FFC approach is the big increase in memory space needed to complete a significant amount of iterations with LS-OPT. The optimization needs the *d3plots* files from the simulations to evaluate the experimental points against the experimental strain field. They can be manually deleted to save disk space, once each iteration analysis is completed. Yet, they do not account for the entire disk space requirements of the iteration, which also lies in several files generated to compare the strain fields. The difference can be around an order of magnitude, or more.

However, the computational cost and the post processing time are substantially equivalent for both methods and the possibility of the FFC approach to compare the strain paths increases the confidence in the accuracy of its results.

4 Failure optimization

The strains measured in all the simulations were higher than those found experimentally. This was due to the complexity of the phenomena that lead to the material failure. It is widely demonstrated in literature that the failure is dependent on the direction of the load even for isotropic steels [10,11]. The material model used in this work is *MAT_024. This material is isotropic with a Von Mises yield surface. To achieve a sufficient accuracy in the failure prediction, the damage and the failure model GISSMO was introduced. It incorporates the load direction variability in the material model using the Triaxiality parameter. Different tensile tests with different triaxialities are needed to accurately tune the parameters of the GISSMO model.
The main equation that rules the accumulation of the damage is [2]:

$$\triangle D = \frac{n}{\epsilon_f(\eta)} \cdot D^{\left(1-\frac{1}{n}\right)} \cdot \triangle \epsilon_{pl} \tag{2}$$

Using the current values of the damage D, of the plastic strain and of the triaxiality, the equation 2 is evaluated at every time step of the simulation and the damage is accumulated. D starts from 0 for every element in the simulation. When the damage in one element reaches unity, the considered element is deleted, as it is unable to support the stress. The possibility to change the value of the damage exponent *n* allows for a non-linear accumulation of the damage. Values of *n* higher than 1 accumulate the damage slowly at the beginning and accelerate the process as D approaches 1. Values of *n* lower than 1 present the opposite behaviour.
Another useful aspect of GISSMO is the introduction of the coupling between the damage and the stress in the element. The damaged elements can withstand less stress than elements without damage. The coupling enables the description of the weakening of the elements. It is implemented in the model with an instability parameter F and its accumulation rule is similar to the equation 2 [2]:

$$\triangle F = \frac{n}{\epsilon_{crit}(\eta)} \cdot F^{\left(1-\frac{1}{n}\right)} \cdot \triangle \epsilon_{pl} \tag{3}$$

When F reaches 1 the coupling begins and the stress supported by the element is reduced as described by the following equation [2]:

$$\sigma = \tilde{\sigma} \cdot \left[1 - \left(\frac{D - D_{crit}}{1 - D_{crit}}\right)^m\right] \tag{4}$$

The optimization is needed to identify the correct combination of values for the damage exponent *n*, the fading exponent *m* and the $\varepsilon_f(\eta)$ *and* $\varepsilon_{crit}(\eta)$. In this work, the two plastic strain curves were discretized with 13 points. Two curves summed to the two exponents to a total of 28 parameters for the optimization, that were reduced to 22 thanks to considerations about the physics of the problem.

4.1 Standard

In this optimization 4 stages are present, one for each of the tested geometry. It was selected a sequential optimization strategy with metamodels generated using a feed-forward neural network Each stage is similar to the ST optimization performed to determine the yield curve: the free parameters are continuously changed, and the engineering force-strain curves of the simulations are compared to the experimental one. At each iteration, LS-OPT improves the metamodel until the desired accuracy is obtained and the optimum combination of the parameters is found. The objectives are multiple, one for each stage and they have the same weight in the optimization. Four constraints were introduced to assure that the instability begun after the necking point.

4.2 Full Field Calibration

The optimization of the full field calibration follows the structure described in the previous section, but it presents a different objective for the four stages. The evaluation of each simulation point is performed by comparing the strain fields, obtained with the simulation and with the experimental tests.

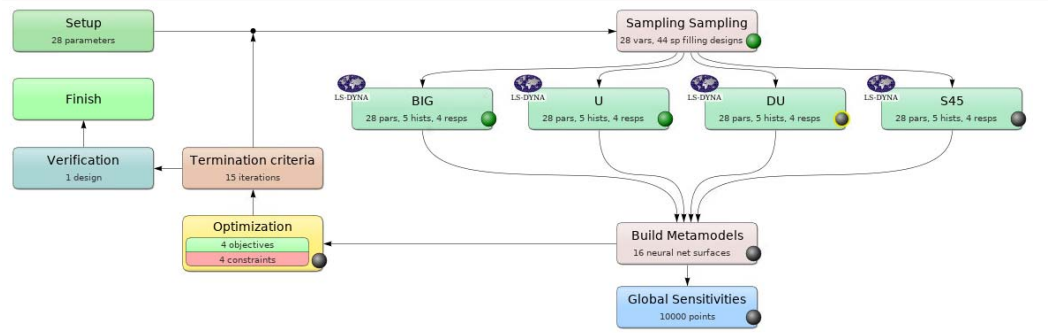

Fig.4: LS-OPT user interface showing the structure used in the ST and FFC GISSMO optimization

4.3 **Results**

The introduction of the GISSMO model brings a better pattern of the behavior of the material in the post-necking phase. This result is present in all the four geometries considered in this work.

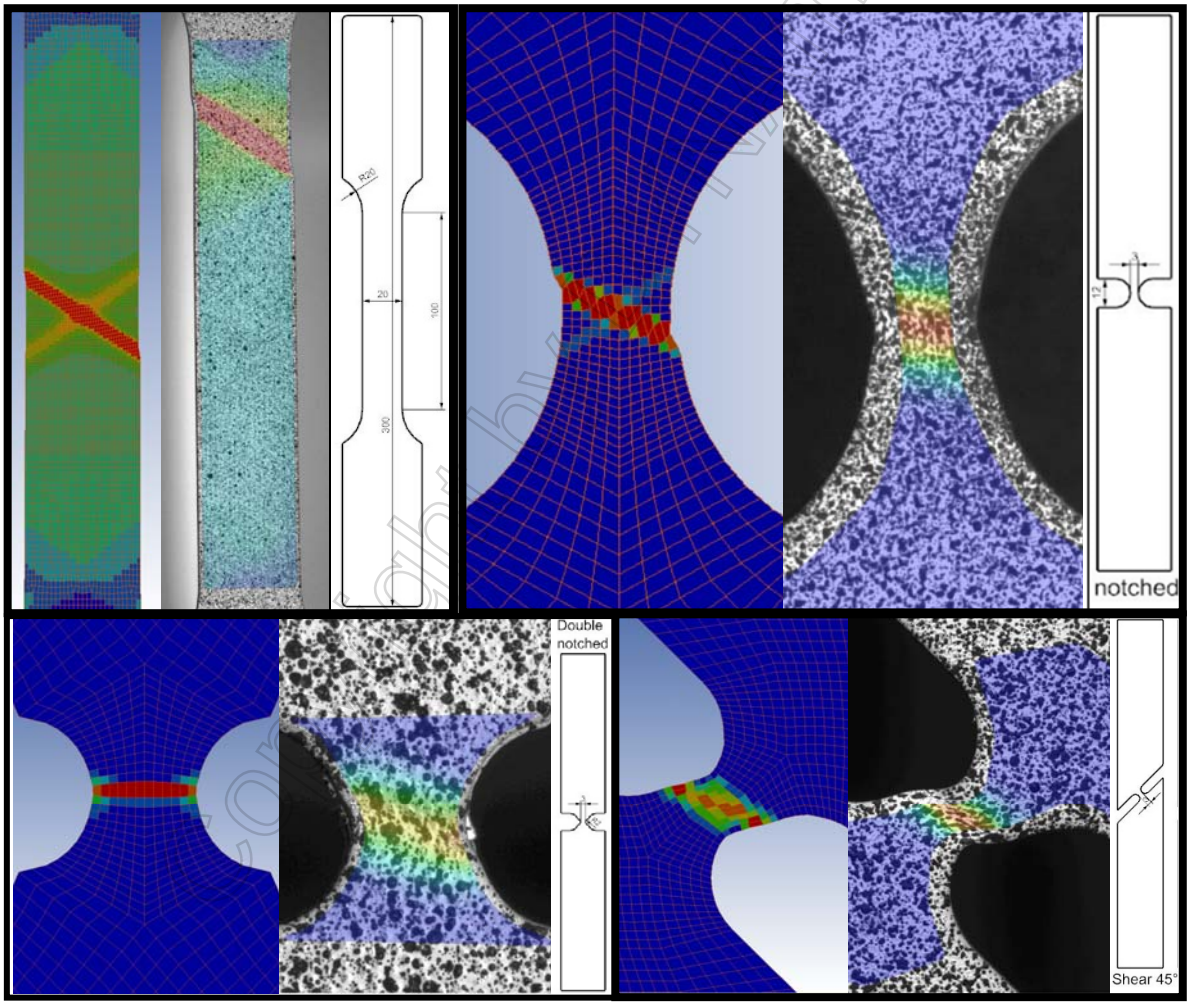

Fig.5: The four geometries' strain fields, as the failure initiates, compared to the experimental strain field. The geometry of the specimens is also shown.

5 Conclusions and future developments

In this work the comparison of two different approaches - Standard and Full Field Calibration - for the calibration of material models was performed. The first approach utilizes the engineering stress-strain curve as evaluation, the second method uses the hyper-curves generated with the digital image correlation. Two metallic materials of quite different characteristics were used in the study: a dual phase DP800 and a martensitic MS1500 steel. The results for both materials lead the authors to

similar conclusions. In terms of results the two methods do not differ significantly, with the FFC approach presenting a better accuracy reproducing the behaviour of the specimens. However, the use of the digital image correlation adds the possibility to compare the actual strain paths to the simulated ones, allowing for a better confidence in the accuracy of the results in exchange for a small cost. A further test on a functional component is suggested to quantify the relevance of the difference in the results from the two approaches.
Furthermore, to progress this work it is crucial to add to the formulation of the *MAT_024 material card the strain rate dependence, which was not included in this work. Regarding the GISSMO parameters, to allow the usage of the calibrated model in commercial simulations - characterized by larger mesh size - the mesh regularization must be performed.

6 Literature

[1] Ilg C. et al., “Application of a Full-Field Calibration Concept for Parameter Identification of HS-Steel with LS-OPT”, 15th Int. LS-Dyna user conference.
[2] F. Andrade et al., “On the Prediction of Material Failure in LS-DYNA®: A Comparison Between GISSMO and DIEM”, 13th Int. LS-Dyna user conference.
[3] A. Haufe et al., “On parameter identification for the GISSMO damage model”, 12th Int. LS-Dyna user conference.
[4] LS-DYNA® user manual
[5] Hockett J.E., Sherby O.D., “Large Strain deformation of polycrystalline metals at low homologous temperatures”, Journal of the Mechanics and Physics of Solids 23, pp. 87-98, 1975.
[6] M. Gonzales, “An inverse methodology for tuning material parameters in numerical modeling of mechanical structures”, Int. Symp. On Solid Mech., 2013
[7] K. Witowski et al., “An Effective Curve Matching Metric for Parameter Identification using Partial Mapping”, 8th European LS-DYNA® Users Conference
[8] LS-OPT® user manual
[9] Strander N. et al., “DIC-based Full-Field Calibration using LS-OPT®: An Update”, 15th Int. LS-Dyna user conference.
[10] Brünig M. et al., “A ductile damage criterion at various stress triaxialities”, Int. J. Plasticity, pp. 1731-1755, 2008.
[11] Lemaitre J., “A Continuous Damage Mechanics Model for Ductile Fracture”, J. Mat. Tech., 107, pp. 83-89, 1985.